Appendix I

MASS SPECTROMETRY DATA ON THE TRIPEPTIDE PRODUCTS OF THE TRANSFERASE REACTION

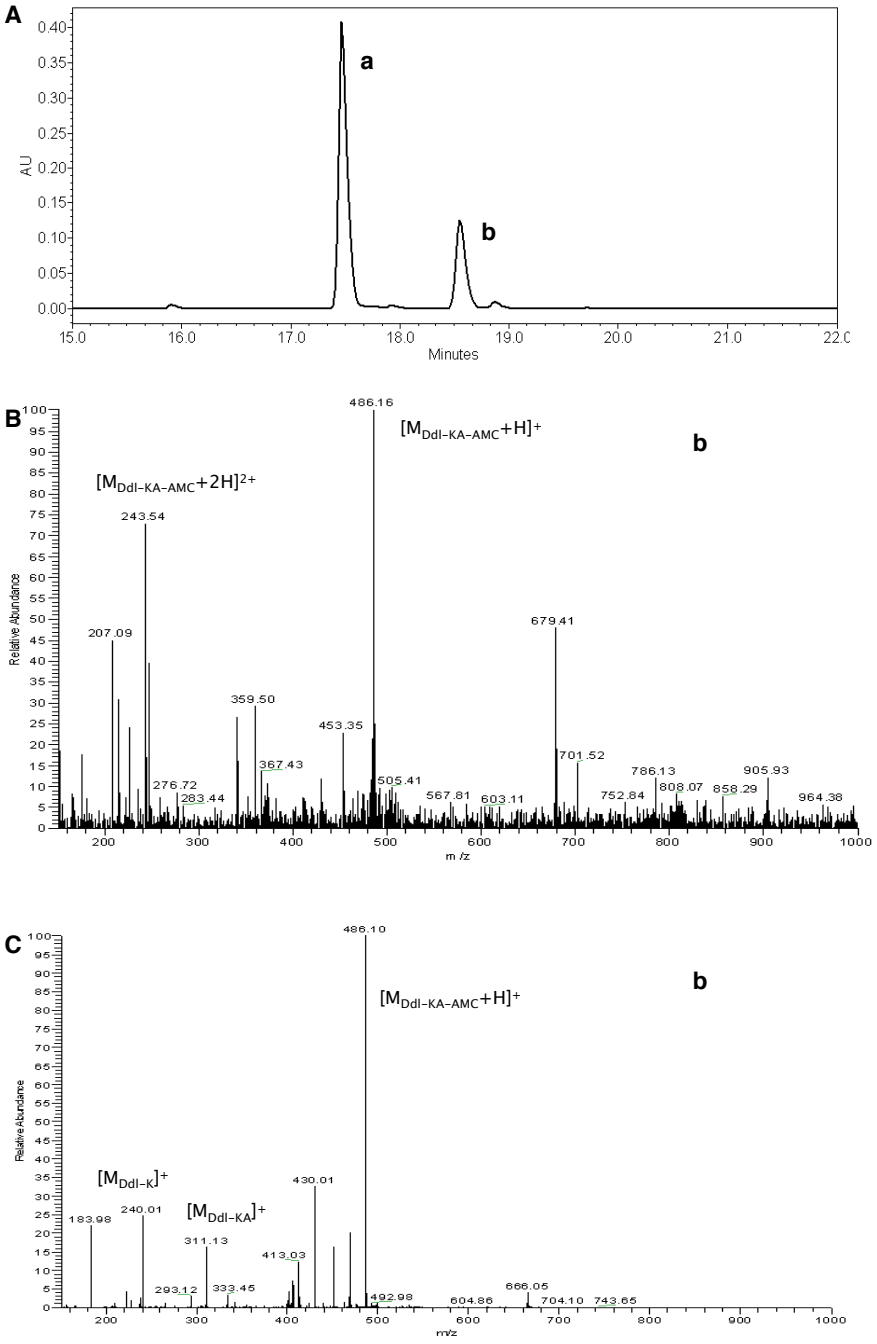

Figure A-1. (A) Representative reversed-phase HPLC analysis of the transfer reaction of dehydroleucine 1 (Ddl) to KA-AMC using UV detection at 324 nm. Both the starting material (a) and the tripeptide product (b) are visible. (B) Analysis of peak (b) by ESI mass spectrometry confirms that it contains the tripeptide product, Ddl-KA-AMC, expecte $[M_{Ddl\text{-}KA\text{-}AMC}+H]^+$ =486.26 m/z and expected$[M_{Ddl\text{-}KA\text{-}AMC}+2H]^{2+}$ =243.63 m/z. (C) MS/MS analysis of the singly-charged ion of the product further confirms the N-terminal addition of Ddl to KA-AMC with fragmentation into dipeptide Ddl-K, $[M_{Ddl\text{-}K}]^+$=240.17 m/z and the tripeptide Ddl-KA, $[M_{Ddl\text{-}KA}]^+$= 311.21 m/z.

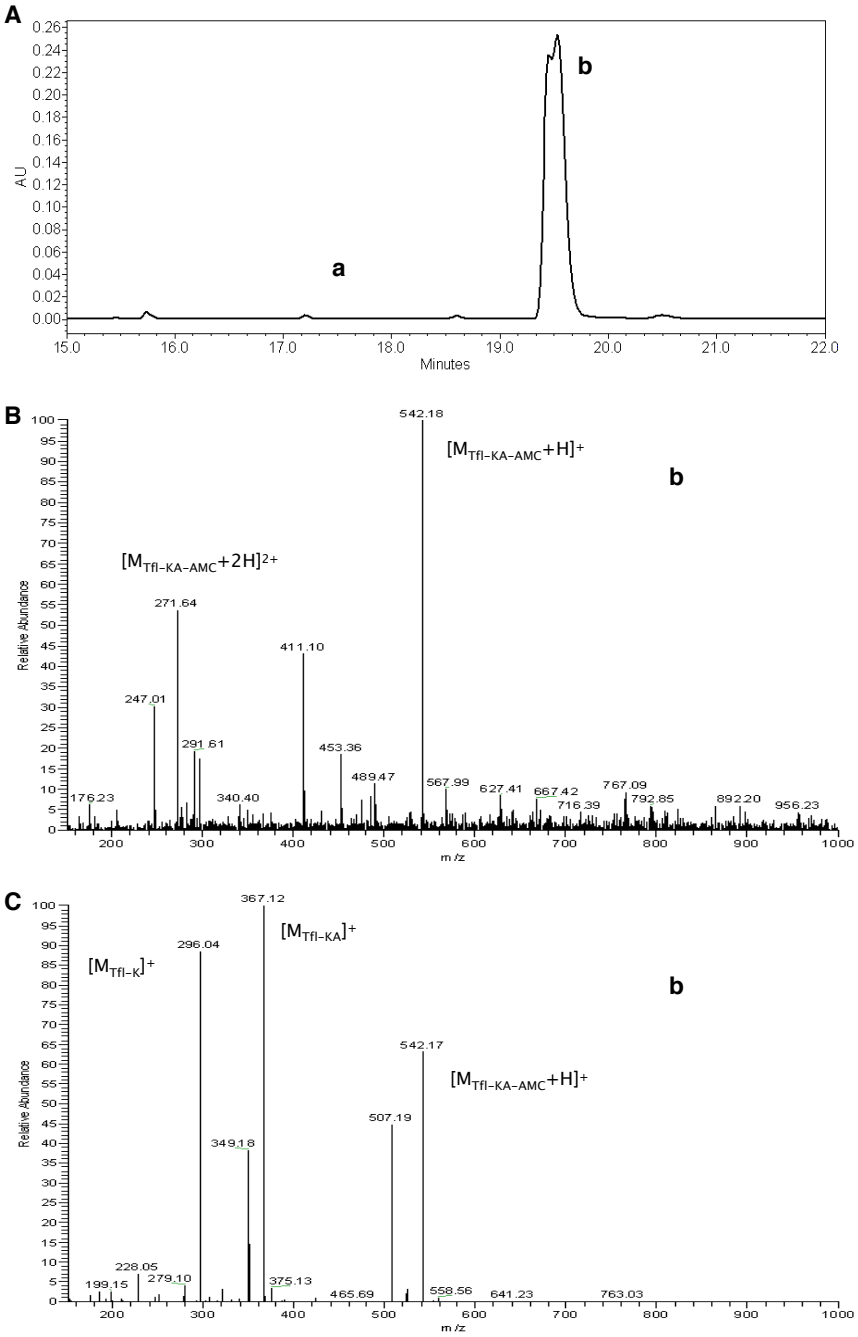

Figure A-2. (A) Representative reversed-phase HPLC analysis of the transfer reaction of trifluoroleucine **2** (Tfl) to KA-AMC using UV detection at 324 nm. The starting material is not detectable at 17.5 minutes and the isomeric product (b) appears at 19.6 minutes. (B) Analysis of peak (b) by ESI mass spectrometry confirms that it contains the tripeptide product, Tfl-KA-AMC, expected $[M_{Tfl\text{-}KA\text{-}AMC}+H]^+$ =542.25 *m/z* and $[M_{Tfl\text{-}KA\text{-}AMC}+2H]^{2+}$ =271.67 *m/z*. (C) MS/MS analysis of the singly-charged ion of the product further confirms the N-terminal addition of Tfl to KA-AMC with fragmentation into dipeptide Tfl-K, expected $[M_{Tfl\text{-}K}]^+$=296.16 *m/z* and the tripeptide Tfl-KA, expected $[M_{Tfl\text{-}KA}]^+$=367.2 *m/z*.

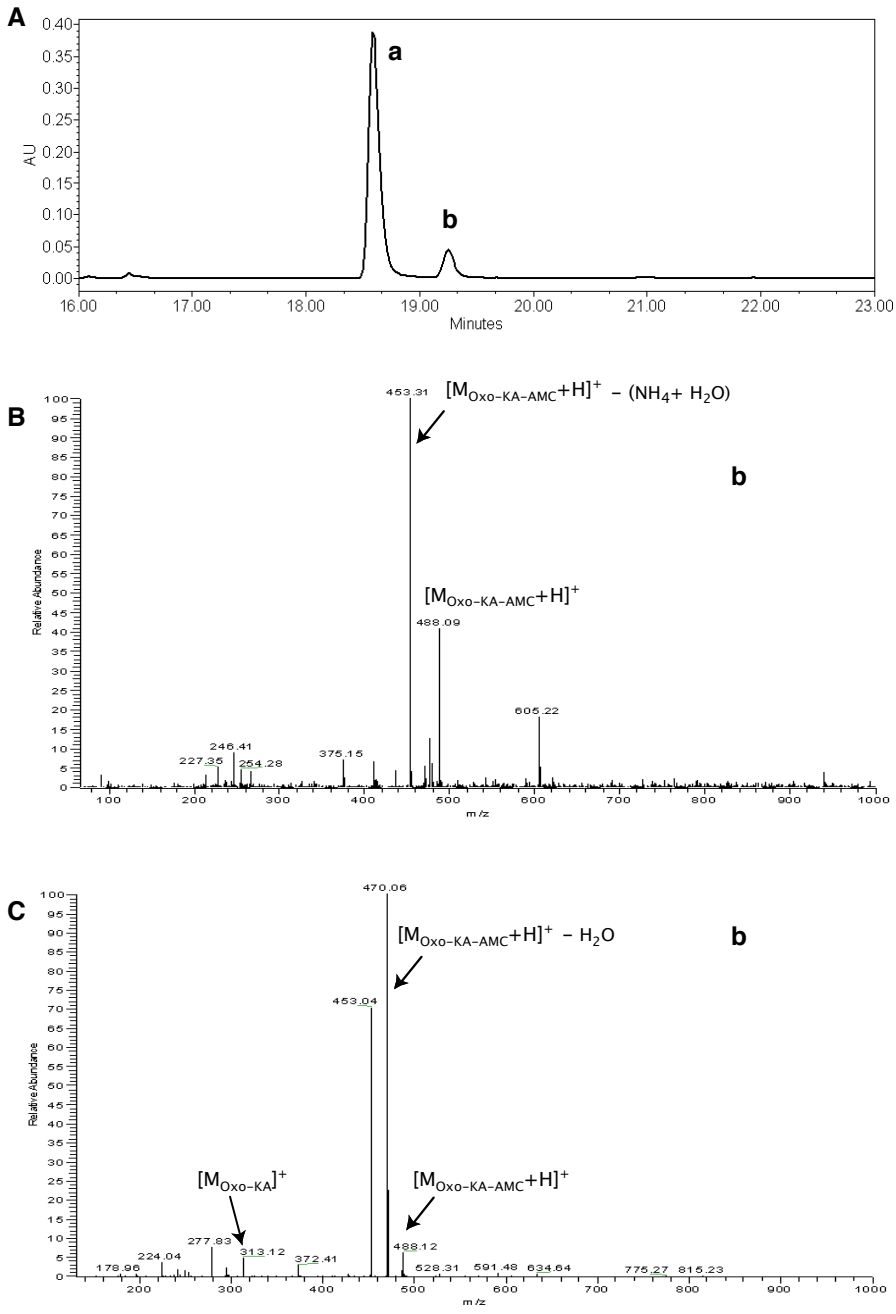

Figure A-3. (A) Representative reversed-phase HPLC analysis of the transfer reaction of oxonorvaline **3** (Oxo) to the dipeptide. Both the starting material (a) and the tripeptide product (b) are visible. (B) The ESI mass spectra of peak (b) confirms that it contains the tripeptide-aminocoumarin product, expected $[M_{Zxo\text{-}KA\text{-}AMC}+H]^+$ = 488.24 *m/z*. (C) Fragmentation of the tripeptide-AMC product ion results in production of the tripeptide ion, Oxo-KA, expected $[M_{Oxo\text{-}KA}]^+$=312.19 *m/z*, as well as loss of water, *m/z* = 470, and ammonium, *m/z* = 453 from the parent ion at 488.12 *m/z*.

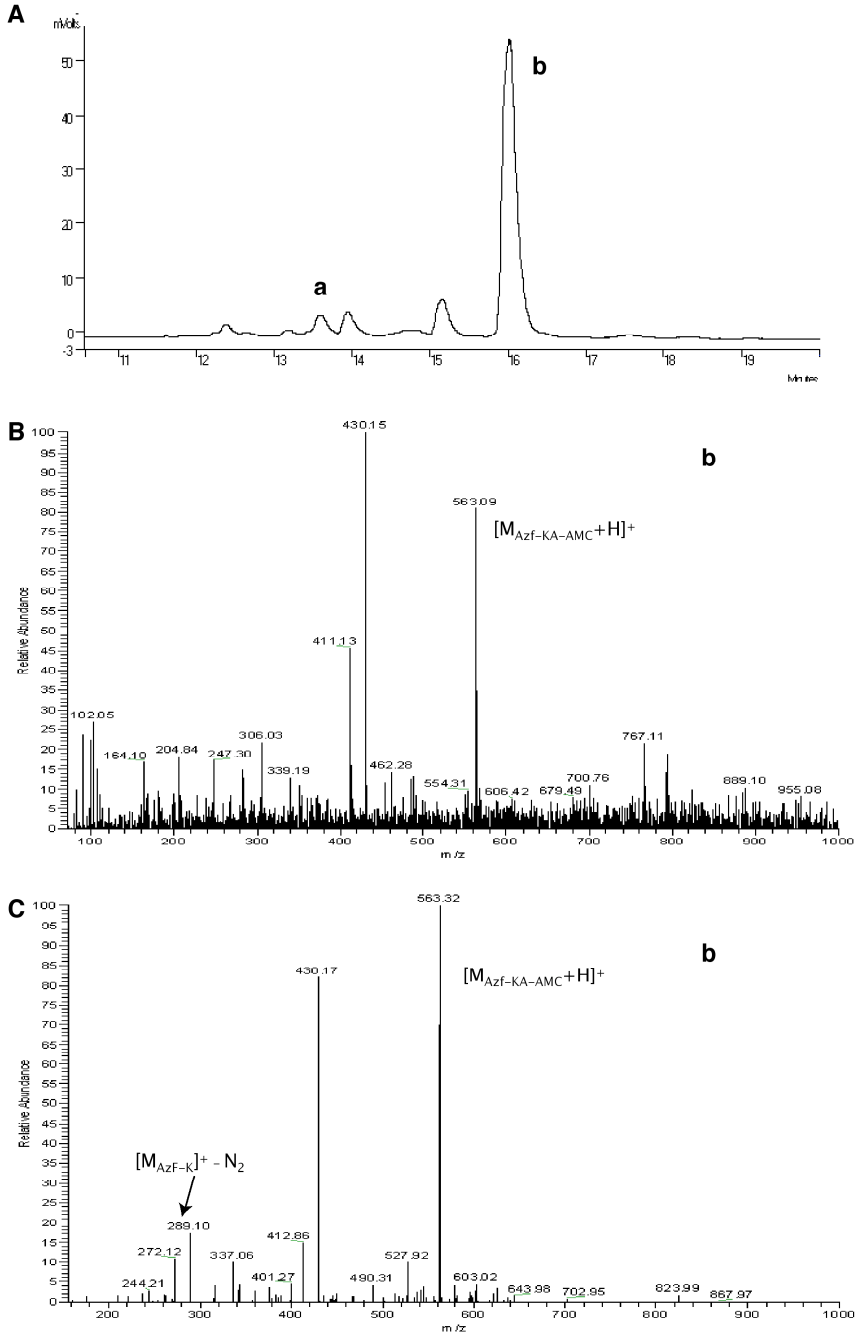

Figure A-4. (A) Representative reversed-phase HPLC analysis of the addition reaction of *p*-azidophenylalanine **4** (Azf) with detection at 324 nm. The retention time of the substrate peak (a) is indicated at 13.5 minutes. The identity of the product peak (b), Azf-KA-AMC, was verified by ESI MS. (B) Analysis of peak (b) by ESI mass spectrometry confirms that it contains the tripeptide product, Azf-KA-AMC, expected $[M_{Azf\text{-}KA\text{-}AMC}+H]^+ = 563.27$ *m/z*. (C) MS/MS analysis of the singly-charged ion of the tripeptide product leads to the loss of dinitrogen from daughter ion Azf-K, expected $[M_{amino\text{-}FK}+H]^+ = 289.18$ *m/z*.

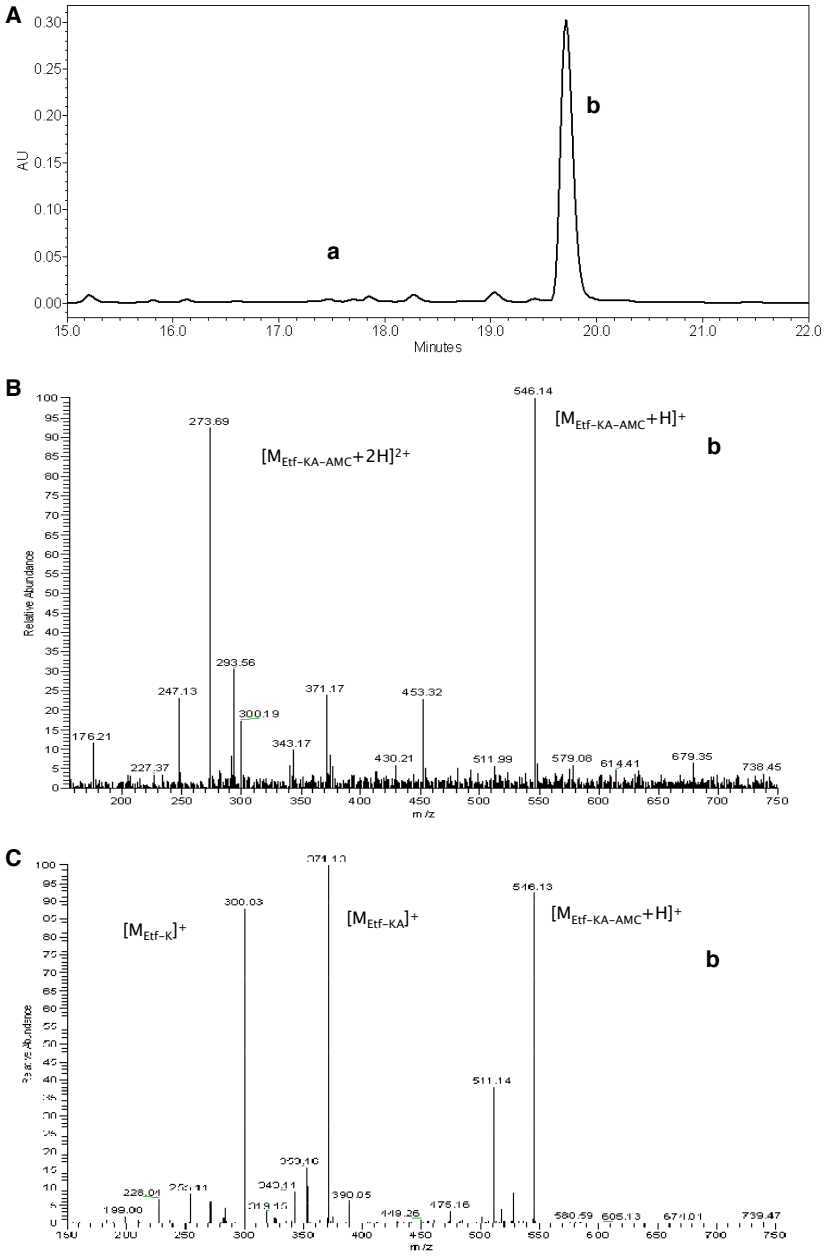

Figure A-5. (A) Representative reversed-phase HPLC analysis of the transfer reaction of *p*-ethynylphenylalanine **5** (Etf) to KA-AMC using UV detection at 324 nm. Only the tripeptide product (b) is visible. (B) Analysis of peak (b) by ESI mass spectrometry confirms that it contains the tripeptide product, Etf-KA-AMC, expected $[M_{Etf\text{-}KA\text{-}AMC}+H]^+$ =546.26 *m/z* and $[M_{Etf\text{-}KA\text{-}AMC}+2H]^{2+}$ = 273.63 *m/z*. (C) MS/MS analysis of the singly-charged ion of the product further confirms the N-terminal addition of Etf to KA-AMC with fragmentation into dipeptide Etf-K, expected $[M_{Etf\text{-}K}]^+$=300.17 *m/z* and the tripeptide Etf-KA, $[M_{Etf\text{-}KA}]^+$= 371.45 *m/z*.

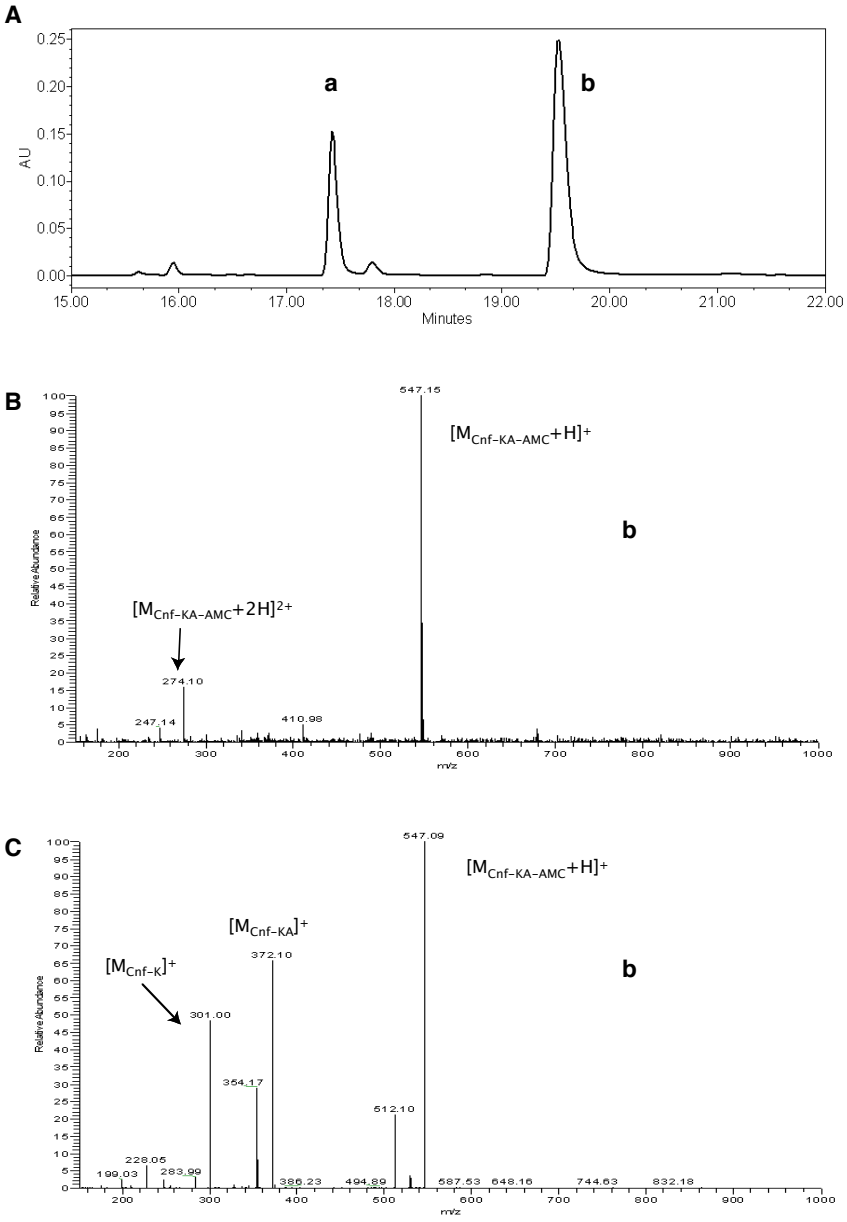

Figure A-6. (A) Representative reversed-phase HPLC analysis of the transfer reaction of *p*-cyanophenylalanine **6** (Cnf) to KA-AMC using UV detection at 324 nm. Both the starting material (a) and the tripeptide product (b) are visible. (B) Analysis of peak (b) by ESI mass spectrometry confirms that it contains the tripeptide product, Cnf-KA-AMC, expected $[M_{Cnf\text{-}KA\text{-}AMC}+H]^+$ = 547.26 *m/z* and $[M_{Cnf\text{-}KA\text{-}AMC}+2H]^{2+}$ =274.23 *m/z*. (C) MS/MS analysis of the singly-charged ion of the product further confirms the N-terminal addition of Cnf to KA-AMC with fragmentation into dipeptide Cnf-K, expected $[M_{Cnf\text{-}K}]^+$=301.17 *m/z* and the tripeptide Cnf-KA, expected $[M_{Cnf\text{-}KA}]^+$= 372.2 *m/z*.

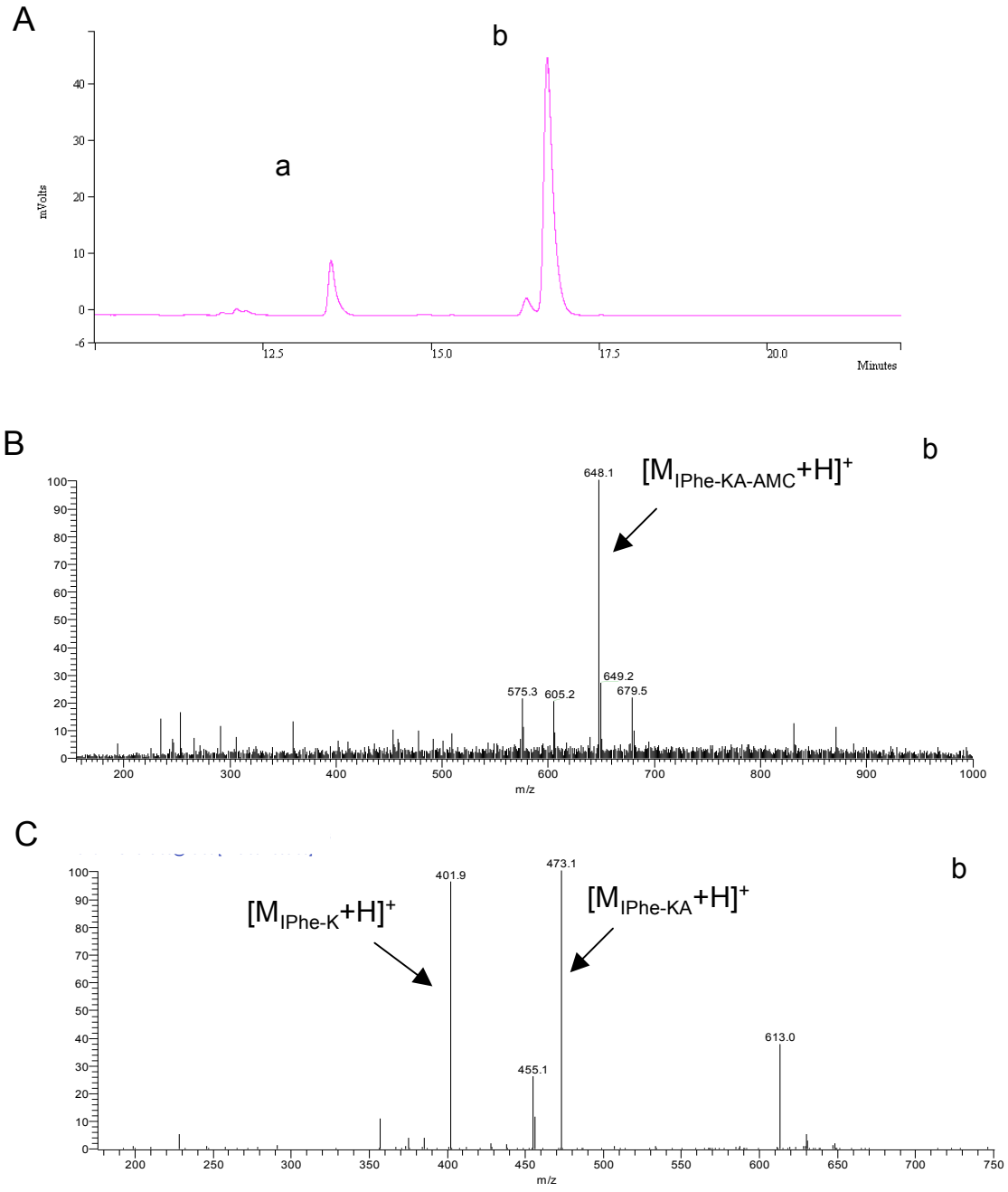

Figure A-7. (A) Representative reversed-phase HPLC analysis of the transfer reaction of *p*-iodophenylalanine **7** (IPhe) to KA-AMC using UV detection at 324 nm. Both the starting material (a) and the tripeptide product (b) are visible. (B) Analysis of peak (b) by ESI mass spectrometry confirms that it contains the tripeptide product, IPhe-KA-AMC, expected $[M_{IPhe\text{-}KA\text{-}AMC}+H]^+ = 648$ *m/z*. (C) MS/MS analysis of the singly-charged ions of the product further confirms the N-terminal addition of IPhe to KA-AMC with fragmentation into the dipeptide, $[M_{IPhe\text{-}K}]^+ = 401$ *m/z* and the tripeptide, $[M_{IPhe\text{-}KA}]^+ = 473.1$ *m/z*.

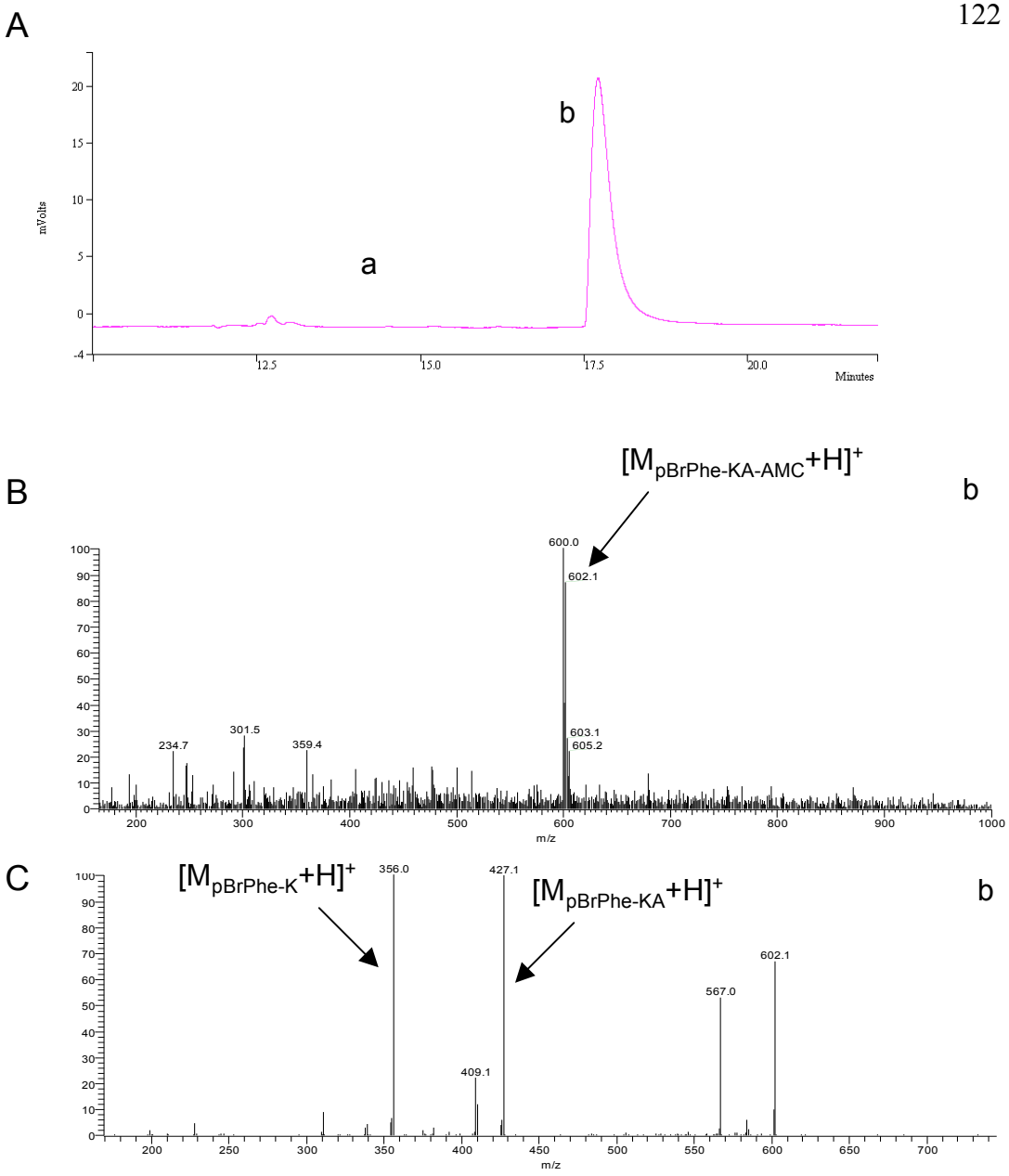

Figure A-8. (A) Representative reversed-phase HPLC analysis of the transfer reaction of p-bromophenylalanine **8** (pBrPhe) to KA-AMC using UV detection at 324 nm. Both the starting material (a) and the tripeptide product (b) are visible. (B) Analysis of peak (b) by ESI mass spectrometry confirms that it contains the tripeptide product, pBrPhe-KA-AMC, expected $[M_{pBrPhe\text{-}KA\text{-}AMC}+H]^+$ = 600 and 602 *m/z* for each of the major isotopes of bromine. (C) MS/MS analysis of the singly-charged ions of the product further confirms the N-terminal addition of pBrPhe to KA-AMC with fragmentation into the dipeptide, $[M_{pBrPhe\text{-}K}]^+$= 356 *m/z* and the tripeptide, $[M_{pBrPhe\text{-}KA}]^+$= 427.1 *m/z*.

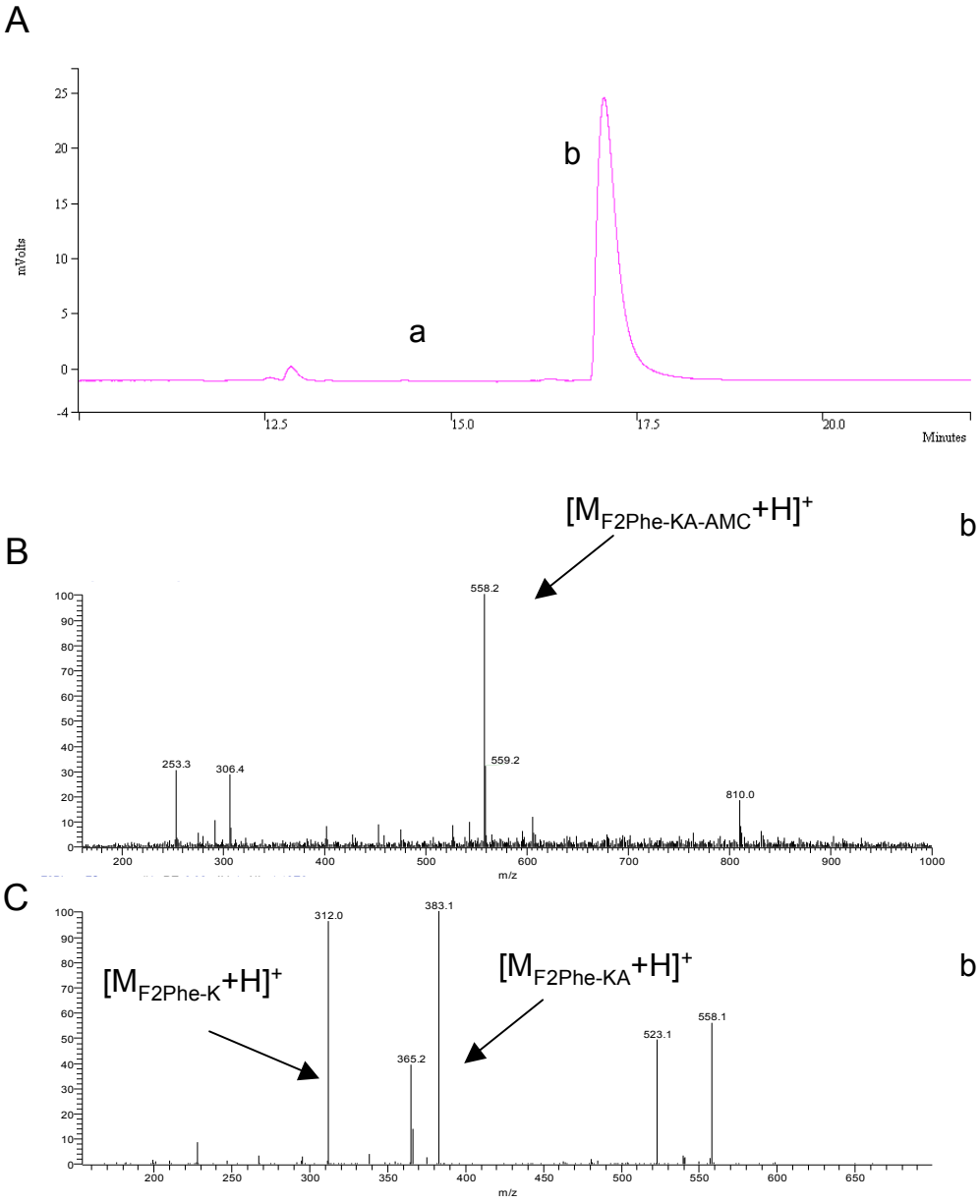

Figure A-9. (A) Representative reversed-phase HPLC analysis of the transfer reaction of 2,3-difluorophenylalanine **9** (F2Phe) to KA-AMC using UV detection at 324 nm. Only the tripeptide product (b) is visible. (B) Analysis of peak (b) by ESI mass spectrometry confirms that it contains the tripeptide product, F2Phe-KA-AMC, expected $[M_{F2Phe\text{-}KA\text{-}AMC}+H]^+ = 558$ *m/z*. (C) MS/MS analysis of the singly-charged ions of the product further confirms the N-terminal addition of F2Phe to KA-AMC with fragmentation into the dipeptide, $[M_{F2Phe\text{-}K}]^+ = 312$ *m/z* and the tripeptide, $[M_{F2Phe\text{-}KA}]^+ = 383.1$ *m/z*.

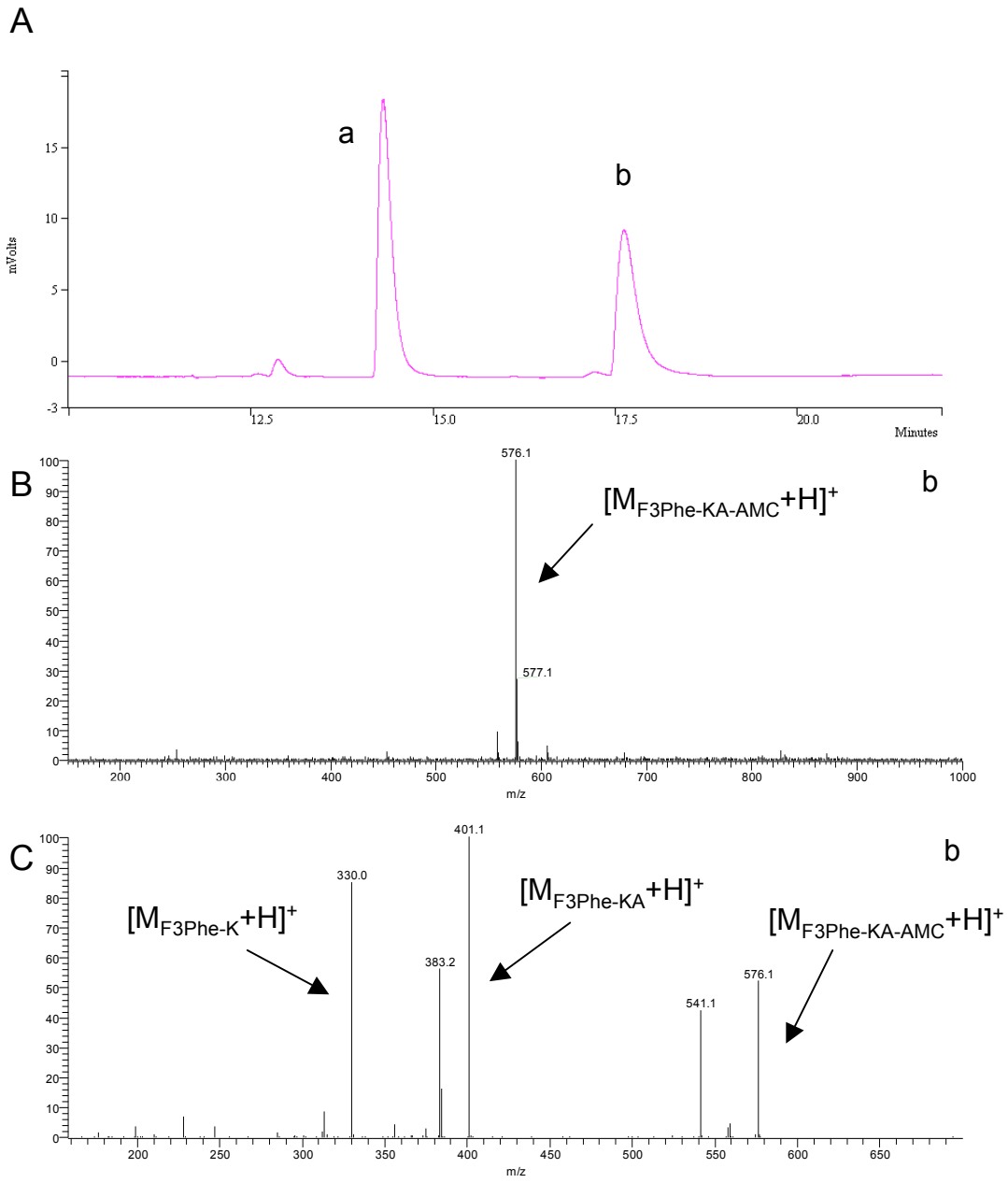

Figure A-10. (A) Representative reversed-phase HPLC analysis of the transfer reaction of 3,4,5-trifluorophenylalanine **10** (F3Phe) to KA-AMC using UV detection at 324 nm. Both the starting material (a) and the tripeptide product (b) are visible. (B) Analysis of peak (b) by ESI mass spectrometry confirms that it contains the tripeptide product, F3Phe-KA-AMC, expected $[M_{F3Phe\text{-}KA\text{-}AMC}+H]^+ = 576$ *m/z*. (C) MS/MS analysis of the singly-charged ions of the product further confirms the N-terminal addition of F3Phe to KA-AMC with fragmentation into the dipeptide, $[M_{F3Phe\text{-}K}]^+ = 330$ *m/z* and the tripeptide, $[M_{F3Phe\text{-}KA}]^+ = 401$ *m/z*.

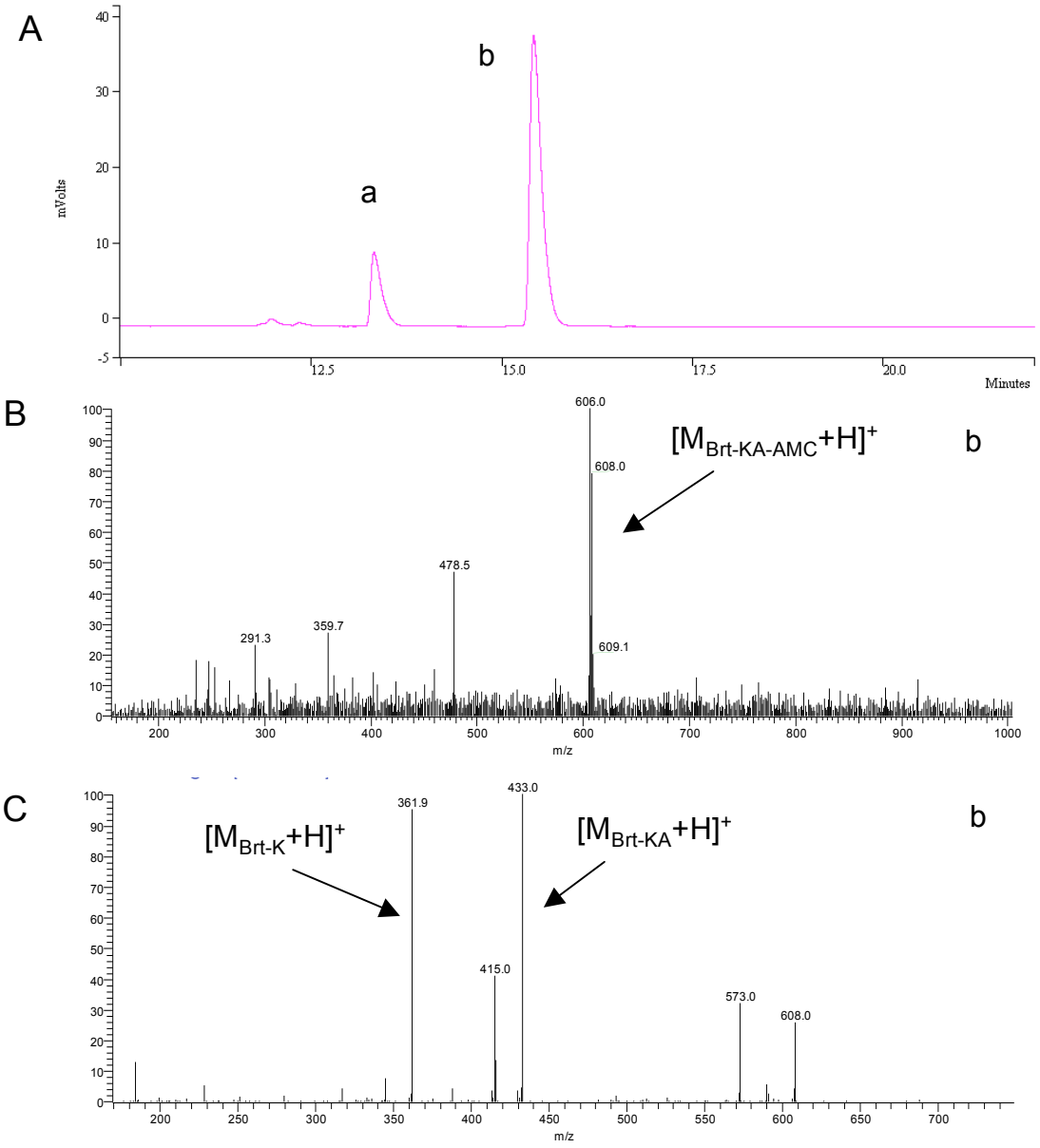

Figure A-11. (A) Representative reversed-phase HPLC analysis of the transfer reaction of 2,5-bromothienylalanine **11** (Brt) to KA-AMC using UV detection at 324 nm. Both the starting material (a) and the tripeptide product (b) are visible. (B) Analysis of peak (b) by ESI mass spectrometry confirms that it contains the tripeptide product, Brt-KA-AMC, expected $[M_{Brt\text{-}KA\text{-}AMC}+H]^+$ = 606 and 608 *m/z* for each of the main isotopes of bromine. (C) MS/MS analysis of the singly-charged ions of the product further confirms the N-terminal addition of Brt to KA-AMC with fragmentation into the dipeptide, $[M_{Brt\text{-}K}]^+$= 361 *m/z* and the tripeptide, $[M_{Brt\text{-}KA}]^+$= 433 *m/z*.

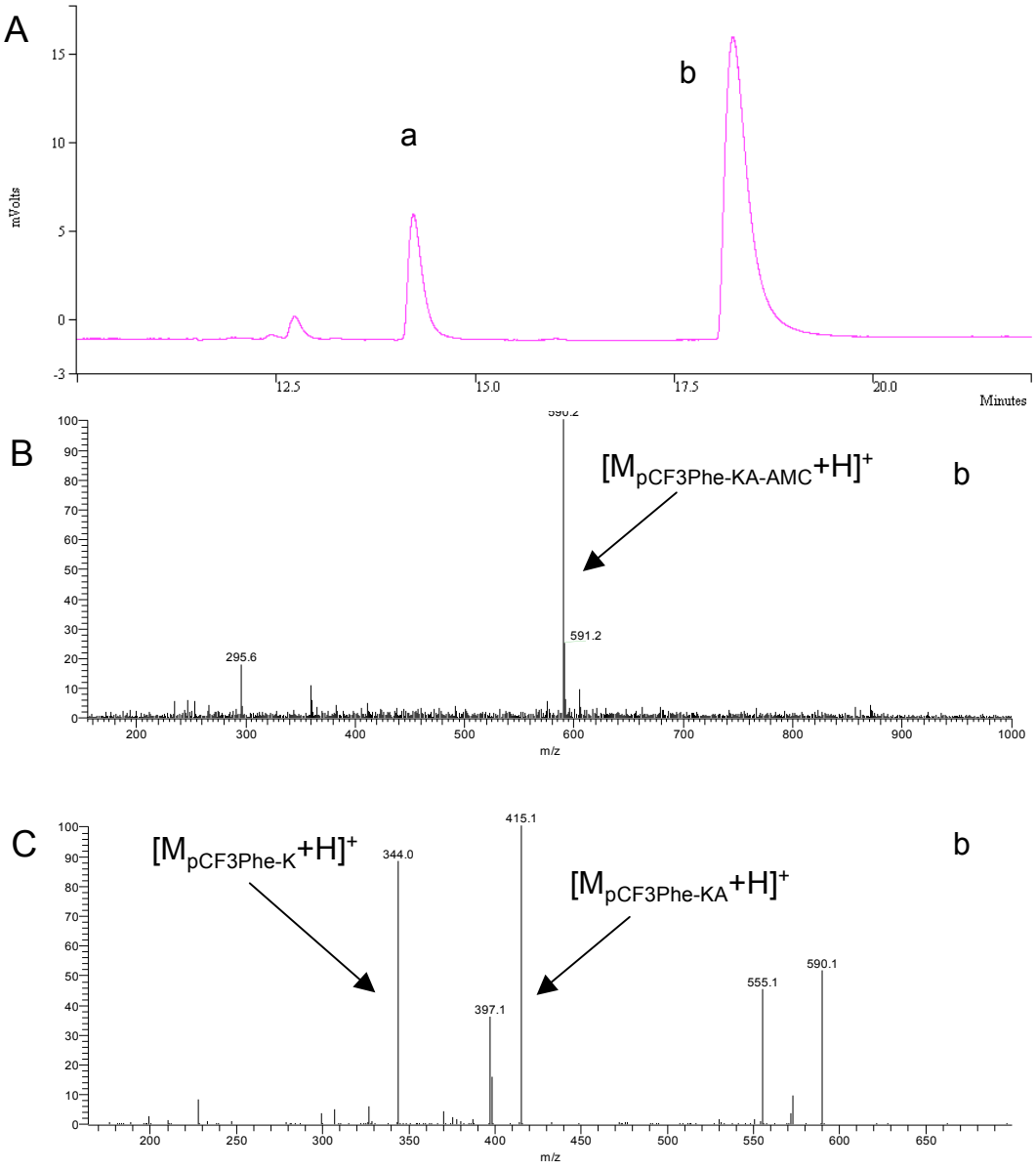

Figure A-12. (A) Representative reversed-phase HPLC analysis of the transfer reaction of *p*-trifluoromethylphenylalanine **12** (pCF3Phe) to KA-AMC using UV detection at 324 nm. Both the starting material (a) and the tripeptide product (b) are visible. (B) Analysis of peak (b) by ESI mass spectrometry confirms that it contains the tripeptide product, pCF3Phe-KA-AMC, expected $[M_{pCF3Phe\text{-}KA\text{-}AMC}+H]^+ = 590.2$ *m/z*. (C) MS/MS analysis of the singly-charged ion of the product further confirms the N-terminal addition of pCF3Phe to KA-AMC with fragmentation into the dipeptide, $[M_{pCF3Phe\text{-}K}]^+=344$ *m/z* and the tripeptide, $[M_{pCF3Phe\text{-}KA}]^+= 415$ *m/z*.

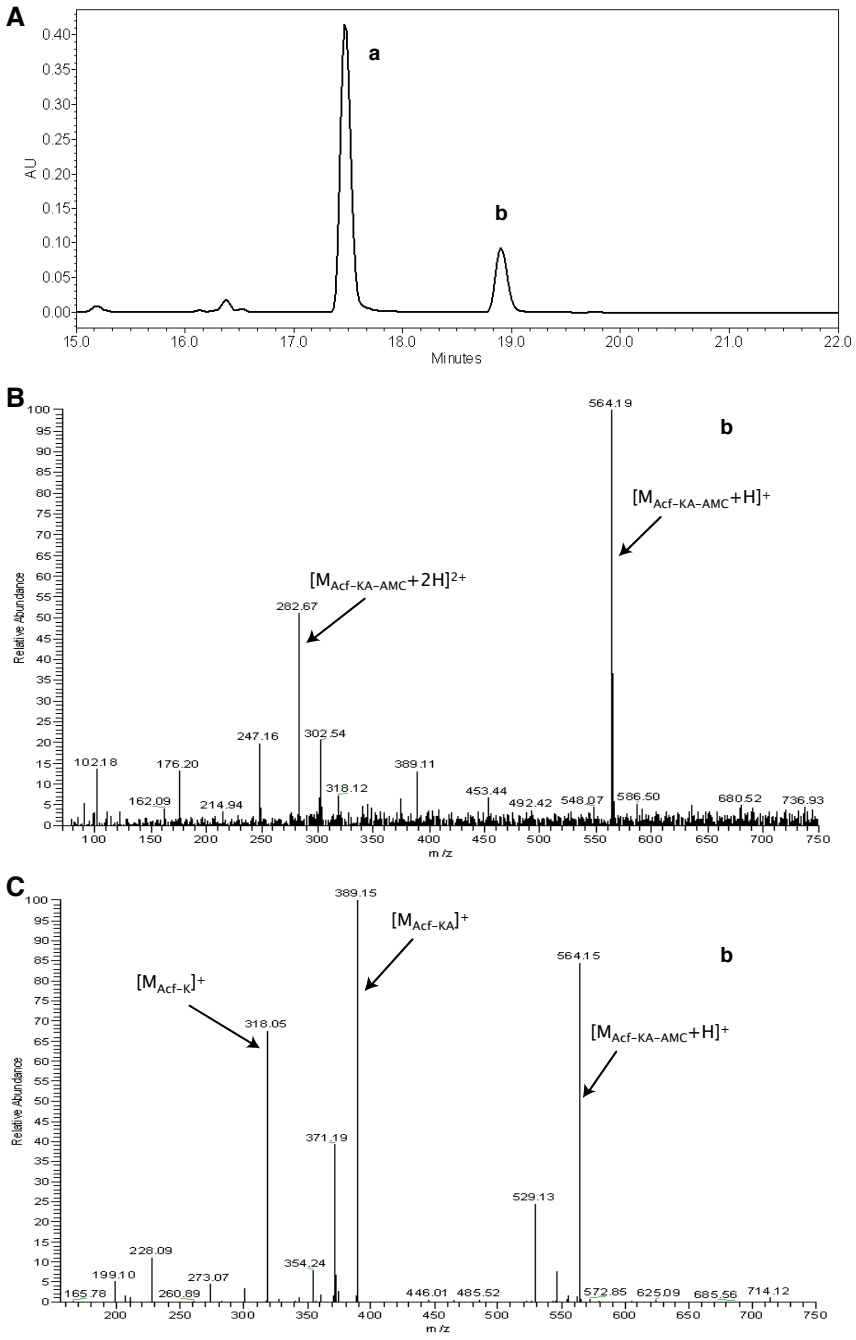

Figure A-13. (A) Representative reversed-phase HPLC analysis of the transfer reaction of *p*-acetylphenylalanine **7** (Acf) to KA-AMC using UV detection at 324 nm. Both the starting material (a) and the tripeptide product (b) are visible. (B) Analysis of peak (b) by ESI mass spectrometry confirms that it contains the tripeptide product, Acf-KA-AMC, expected $[M_{Acf\text{-}KA\text{-}AMC}+H]^+$ =564.27 *m/z* and $[M_{Acf\text{-}KA\text{-}AMC}+2H]^{2+}$ =282.64 *m/z*. (C) MS/MS analysis of the singly-charged ion of the product further confirms the N-terminal addition of Acf to KA-AMC with fragmentation into dipeptide Acf-K, $[M_{Ddl\text{-}K}]^+$=318.18 *m/z* and the tripeptide Acf-KA, $[M_{Acf\text{-}KA}]^+$= 389.22 *m/z*.

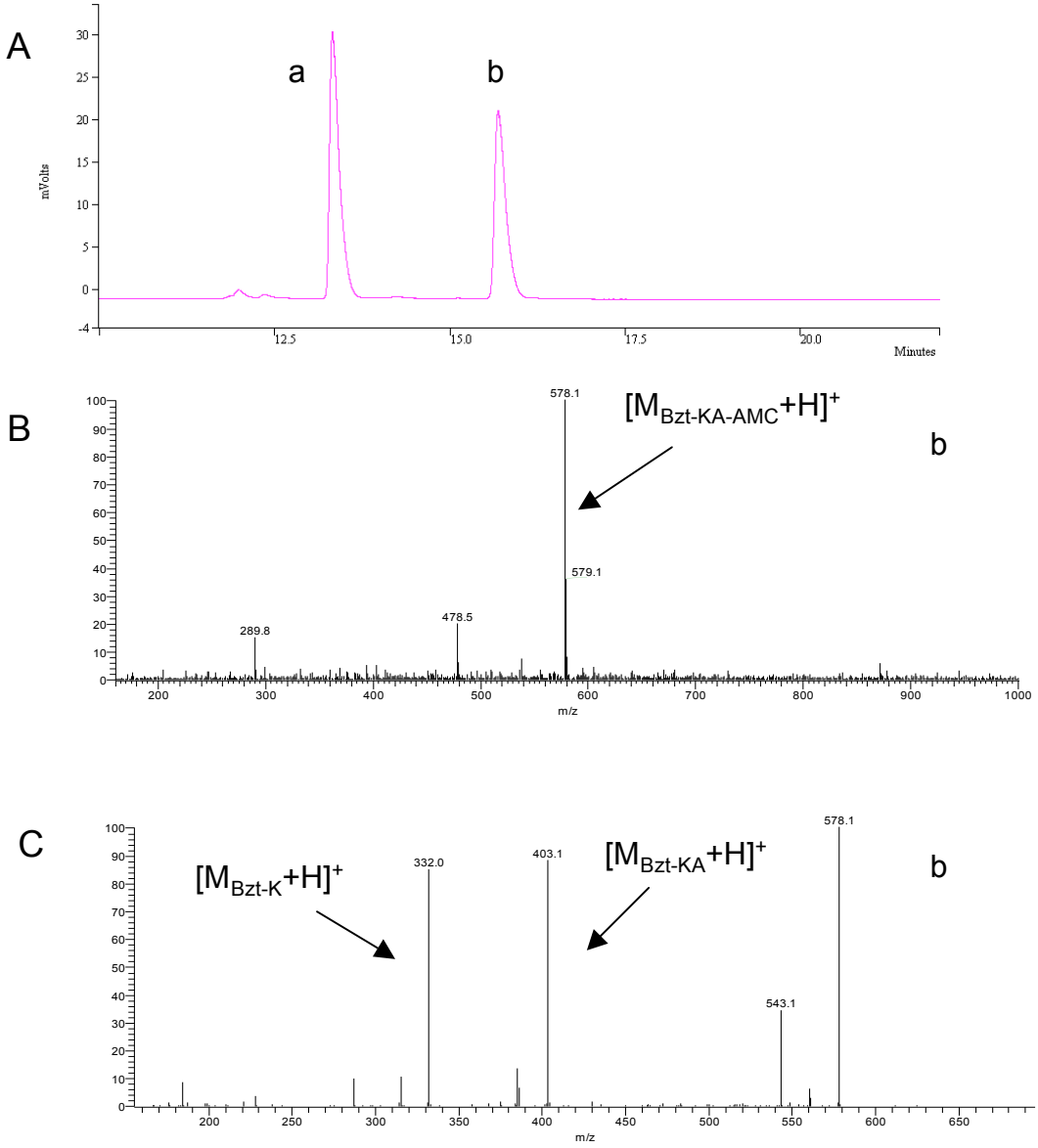

Figure A-14. (A) Representative reversed-phase HPLC analysis of the transfer reaction of benzothienylalanine **14** (Bzt) to KA-AMC using UV detection at 324 nm. Both the starting material (a) and the tripeptide product (b) are visible. (B) Analysis of peak (b) by ESI mass spectrometry confirms that it contains the tripeptide product, Bzt-KA-AMC, expected $[M_{Bzt\text{-}KA\text{-}AMC}+H]^+$ = 578 *m/z*. (C) MS/MS analysis of the singly-charged ion of the product further confirms the N-terminal addition of Bzt to KA-AMC with fragmentation into the dipeptide, $[M_{Bzt\text{-}K}]^+$=403.1 *m/z* and the tripeptide, $[M_{Bzt\text{-}KA}]^+$= 332 *m/z*.

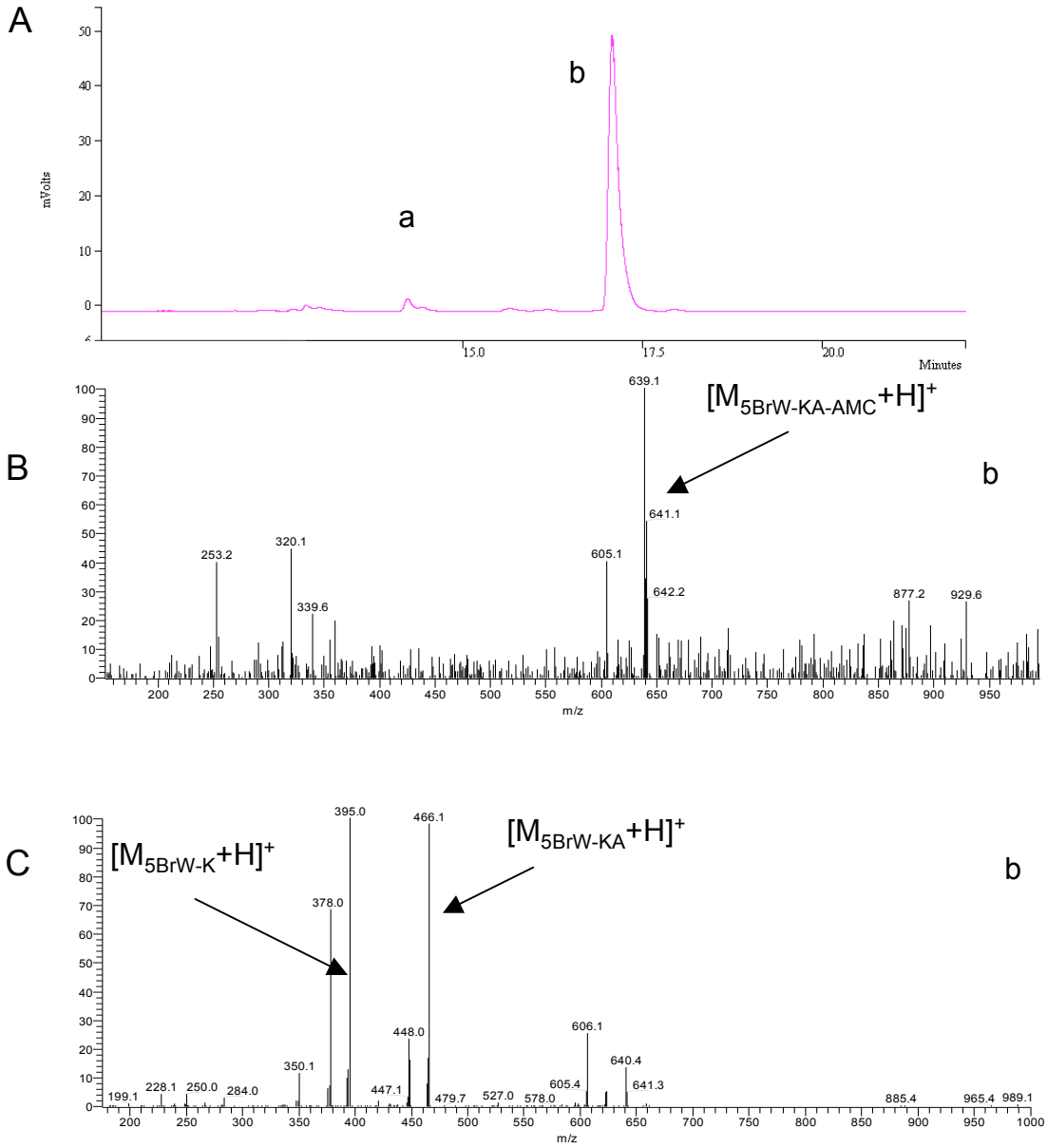

Figure A-15. (A) Representative reversed-phase HPLC analysis of the transfer reaction of 5-bromotryptophan **15** (5BrW) to KA-AMC using UV detection at 324 nm. Only the tripeptide product (b) is visible. (B) Analysis of peak (b) by ESI mass spectrometry confirms that it contains the tripeptide product, 5BrW-KA-AMC, expected $[M_{5BrW\text{-}KA\text{-}AMC}+H]^+$ = 639 and 641 *m/z* for each of the main isotopes of bromine. (C) MS/MS analysis of the singly-charged ion of the product further confirms the N-terminal addition of 5BrW to KA-AMC with fragmentation into the dipeptide, $[M_{5BrW\text{-}K}]^+$=466.1 *m/z* and the tripeptide, $[M_{5BrW\text{-}KA}]^+$= 395 *m/z*.

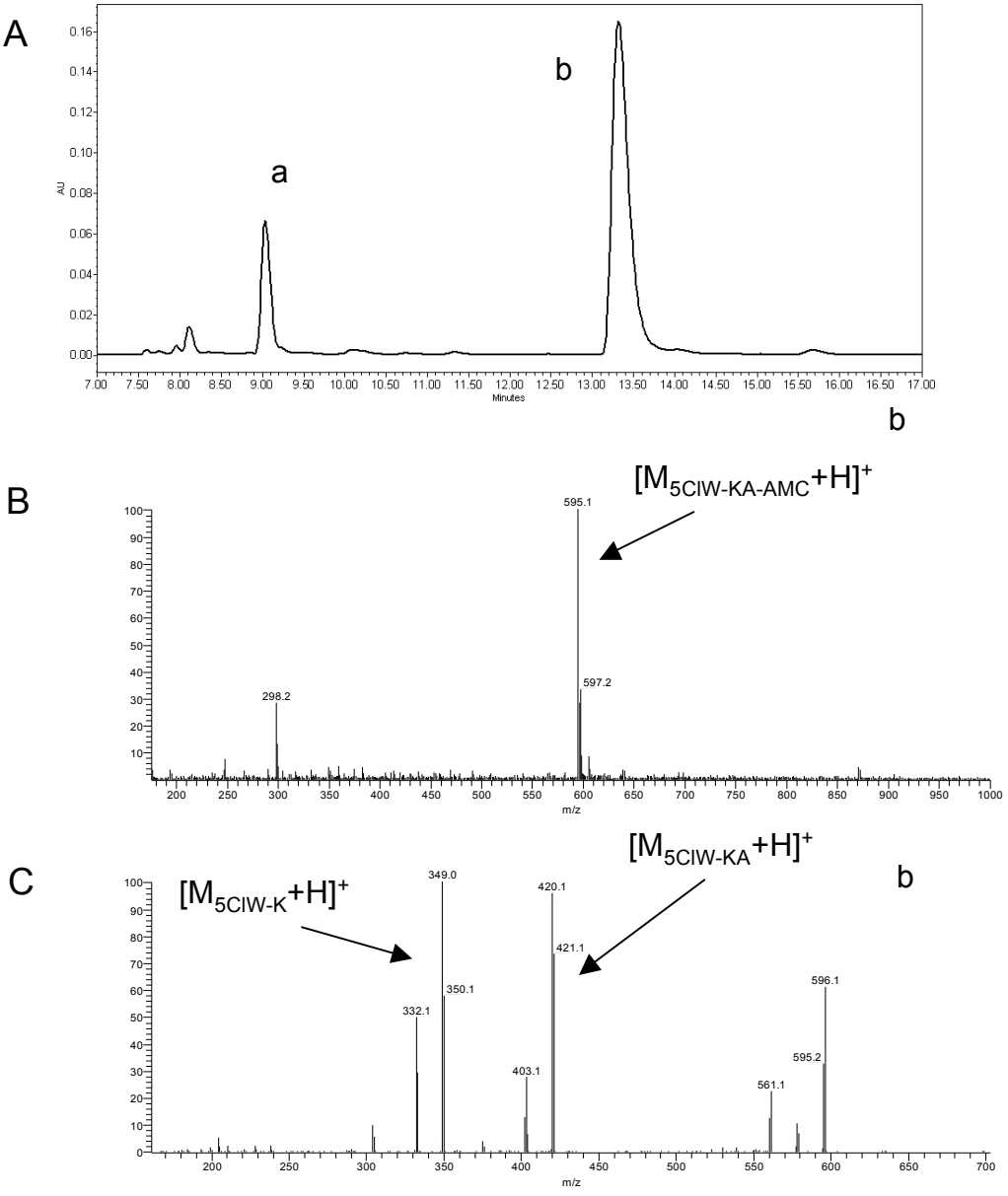

Figure A-16. (A) Representative reversed-phase HPLC analysis of the transfer reaction of 5-chlorotryptophan **16** (5ClW) to KA-AMC using UV detection at 324 nm. Both the starting material (a) and the tripeptide product (b) are visible. (B) Analysis of peak (b) by ESI mass spectrometry confirms that it contains the tripeptide product, 5ClW-KA-AMC, expected $[M_{5ClW\text{-}KA\text{-}AMC}+H]^+$ = 595.1 *m/z* and $[M_{5ClW\text{-}KA\text{-}AMC}+2H]^{2+}$ = 298.1 *m/z*. (C)) MS/MS analysis of the singly-charged ion of the product further confirms the N-terminal addition of 5ClW to KA-AMC with fragmentation into the dipeptide, $[M_{5ClW\text{-}K}]^+$=349 *m/z* and the tripeptide, $[M_{5ClW\text{-}KA}]^+$= 420.1 *m/z*.

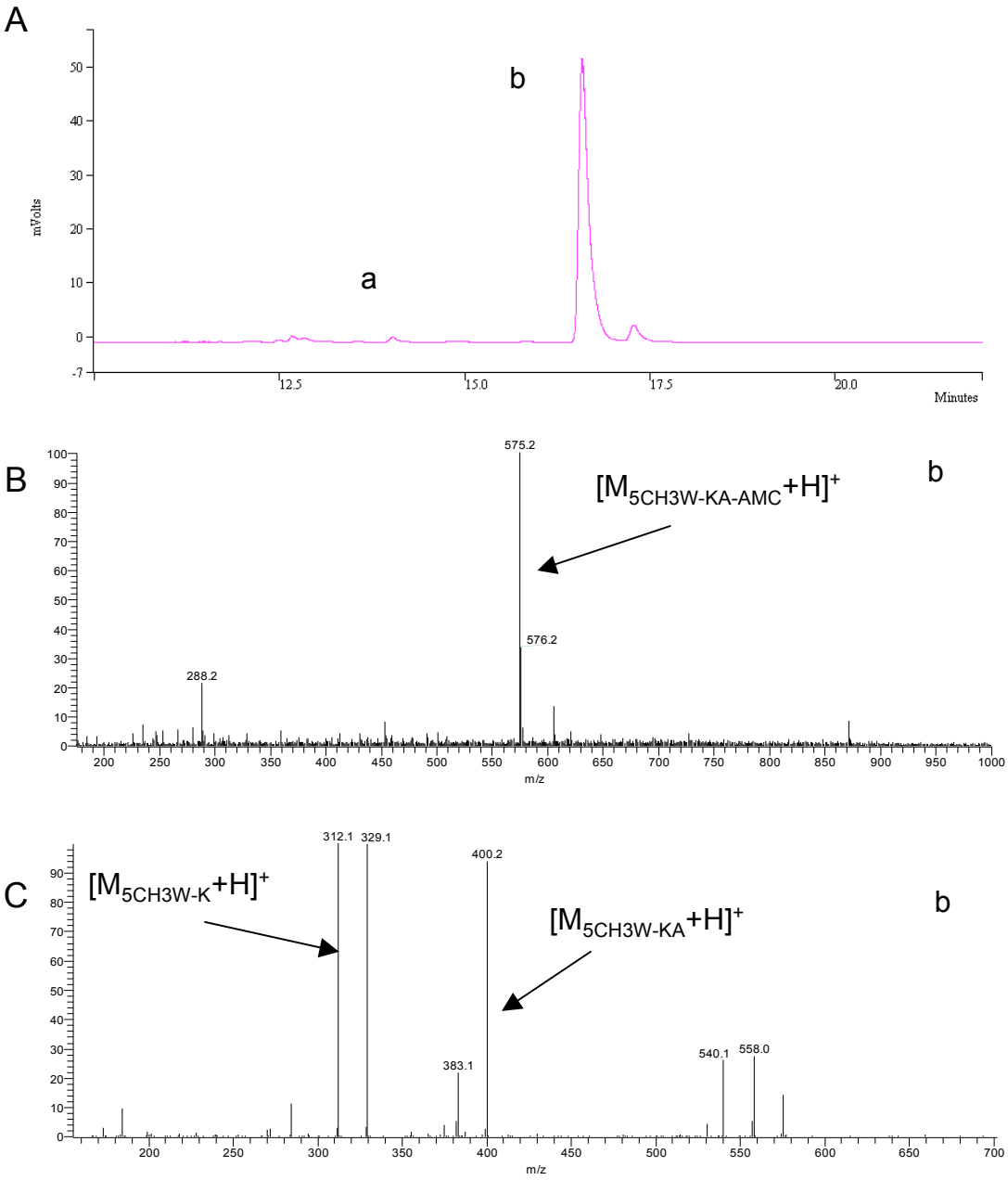

Figure A-17. (A) Representative reversed-phase HPLC analysis of the transfer reaction of 5-methyltryptophan **17** (5CH3W) to KA-AMC using UV detection at 324 nm. Only the tripeptide product (b) is visible. (B) Analysis of peak (b) by ESI mass spectrometry confirms that it contains the tripeptide product, 5CH3W-KA-AMC, expected $[M_{5CH3W\text{-}KA\text{-}AMC}+H]^+ = 575$ *m/z* and $[M_{5CH3W\text{-}KA\text{-}AMC}+2H]^{2+} = 288.3$ *m/z*. (C) MS/MS analysis of the singly-charged ion of the product further confirms the N-terminal addition of 5CH3W to KA-AMC with fragmentation into dipeptide, $[M_{5CH3W\text{-}K}]^+ = 329.1$ *m/z* and the tripeptide, $[M_{5CH3W\text{-}KA}]^+ = 400.2$ *m/z*.

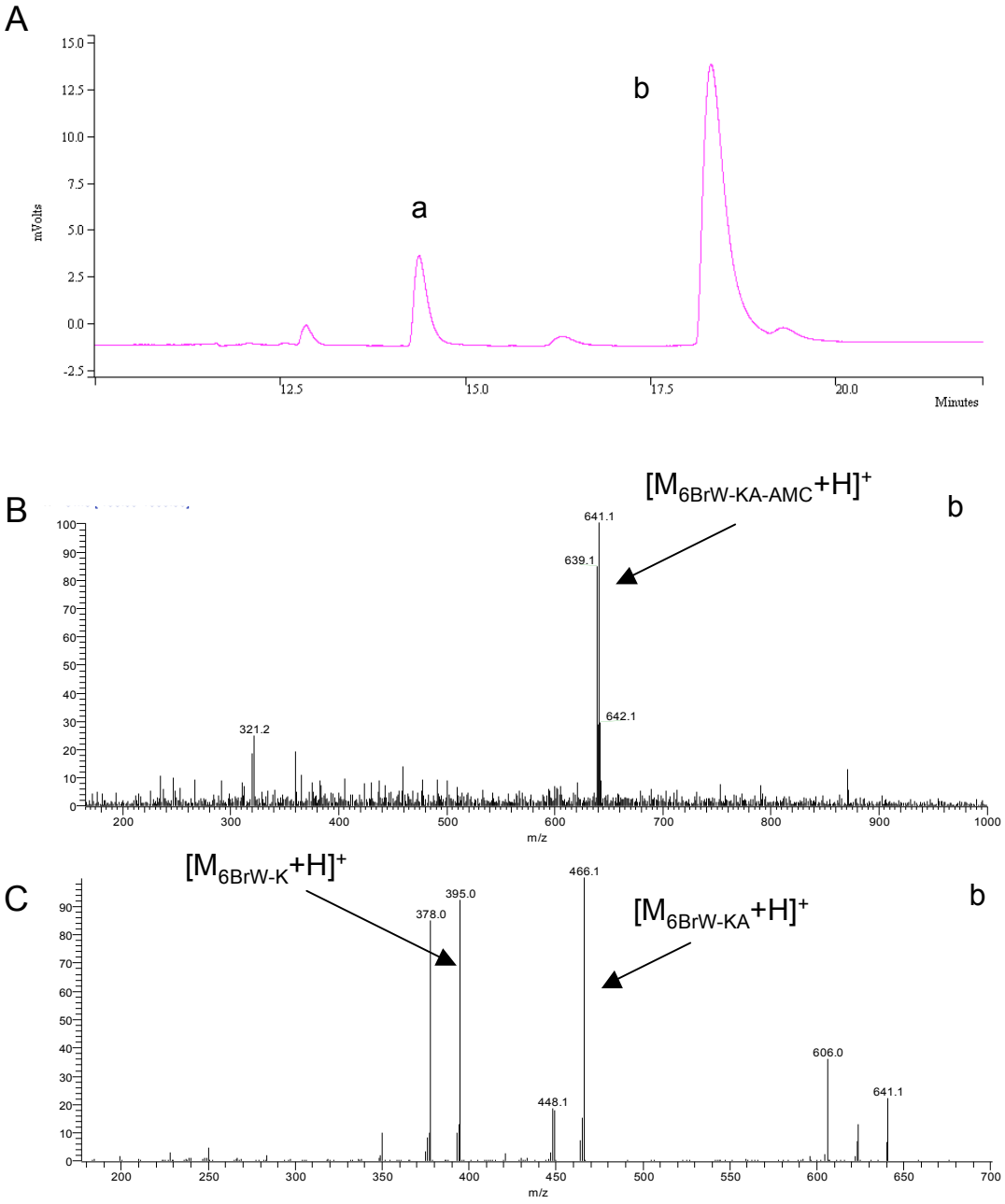

Figure A-18. (A) Representative reversed-phase HPLC analysis of the transfer reaction of 6-bromotryptophan **19** (6BrW) to KA-AMC using UV detection at 324 nm. Both the starting material (a) and the tripeptide product (b) are visible. (B) Analysis of peak (b) by ESI mass spectrometry confirms that it contains the tripeptide product, 6BrW-KA-AMC, expected $[M_{6BrW\text{-}KA\text{-}AMC}+H]^+$ = 639 and 641 *m/z* for each of the main isotopes of bromine. (C) MS/MS analysis of the singly-charged ion of the product further confirms the N-terminal addition of 6BrW to KA-AMC with fragmentation into the dipeptide, $[M_{6BrW\text{-}K}]^+$= 395.0 *m/z* and the tripeptide, $[M_{6BrW\text{-}KA}]^+$= 466.1 *m/z*.

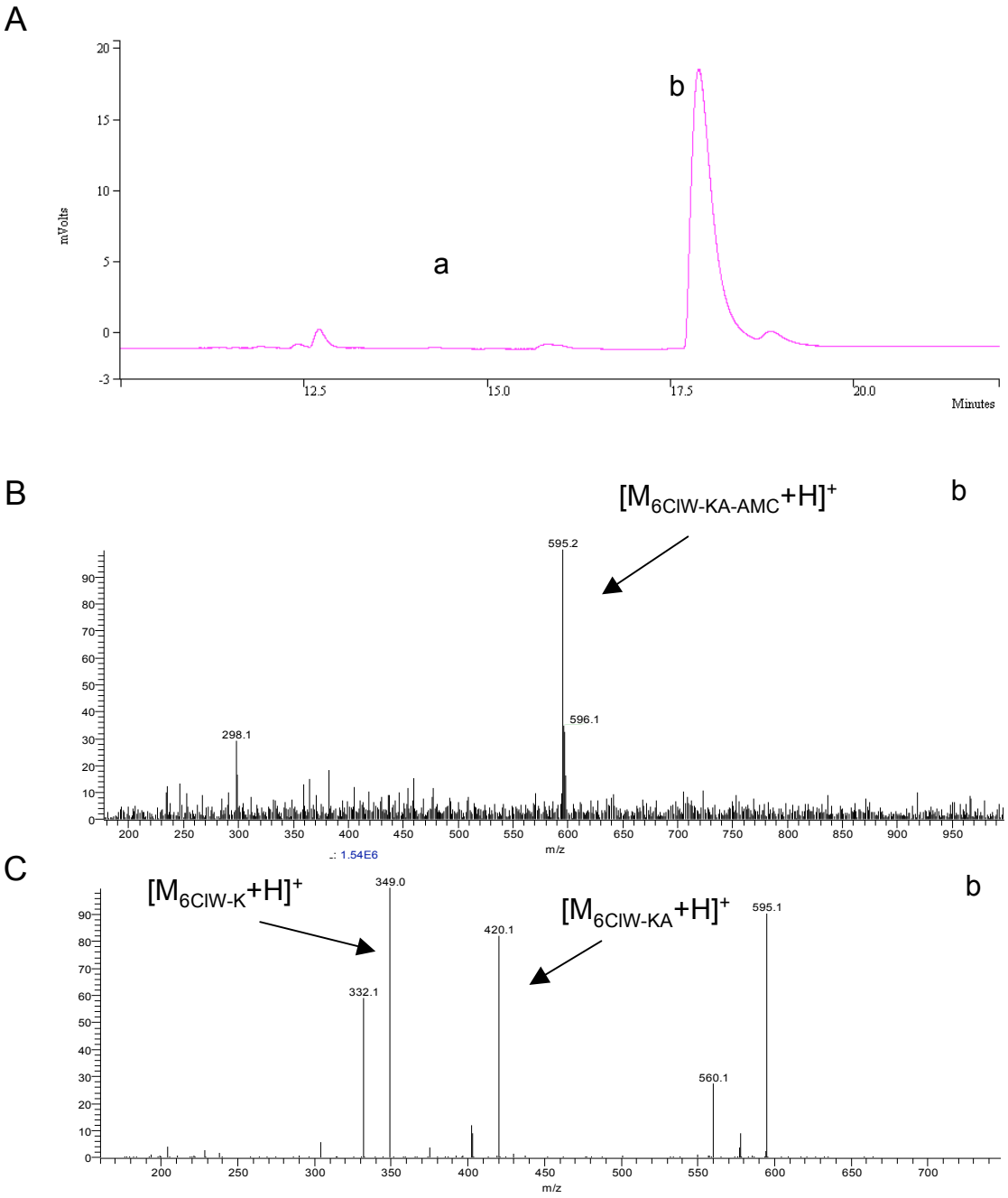

Figure A-19. (A) Representative reversed-phase HPLC analysis of the transfer reaction of 6-chlorotryptophan **19** (6ClW) to KA-AMC using UV detection at 324 nm. Only the tripeptide product (b) is visible. (B) Analysis of peak (b) by ESI mass spectrometry confirms that it contains the tripeptide product, 6ClW-KA-AMC, expected $[M_{6ClW\text{-}KA\text{-}AMC}+H]^+$ = 595.1 *m/z* and $[M_{6ClW\text{-}KA\text{-}AMC}+2H]^{2+}$ = 298.1 *m/z*. (C)) MS/MS analysis of the singly-charged ion of the product further confirms the N-terminal addition of 6ClW to KA-AMC with fragmentation into the dipeptide, $[M_{6ClW\text{-}K}]^+$=349 *m/z* and the tripeptide, $[M_{6ClW\text{-}KA}]^+$= 420.1 *m/z*.

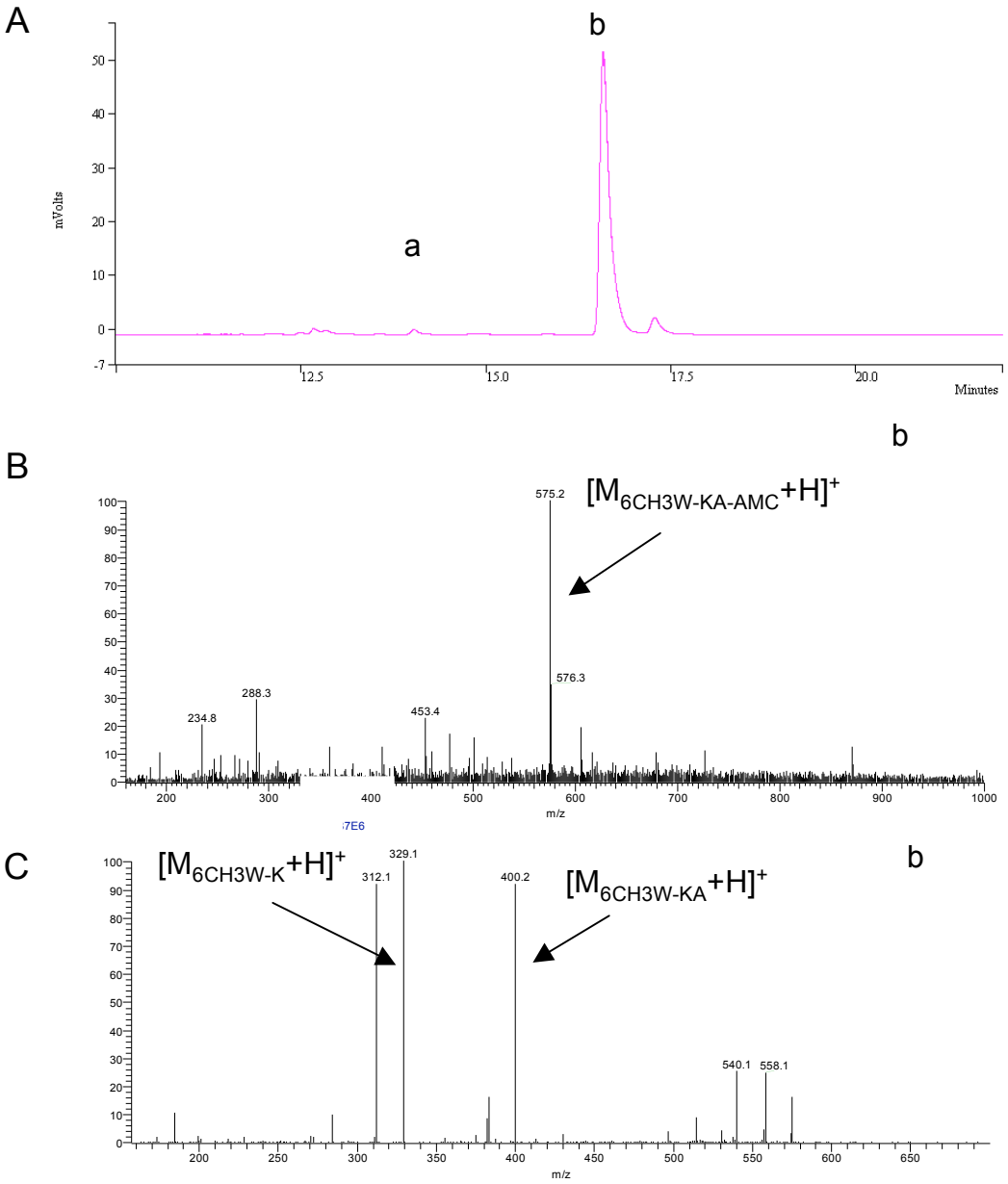

Figure A-20. (A) Representative reversed-phase HPLC analysis of the transfer reaction of 6-methylryptophan **20** (6CH3W) to KA-AMC using UV detection at 324 nm. Only the tripeptide product (b) is visible. (B) Analysis of peak (b) by ESI mass spectrometry confirms that it contains the tripeptide product, 6CH3W-KA-AMC, expected $[M_{6CH3W\text{-}KA\text{-}AMC}+H]^+$ = 575 *m/z* and $[M_{6CH3W\text{-}KA\text{-}AMC}+2H]^{2+}$ =288.3 *m/z*. (C) MS/MS analysis of the singly-charged ion of the product further confirms the N-terminal addition of 6CH3W to KA-AMC with fragmentation into dipeptide 6CH3W-K, $[M_{6CH3W\text{-}K}]^+$=329.1 *m/z* and the tripeptide 6CH3W-KA, $[M_{6CH3W\text{-}KA}]^+$= 400.2 *m/z*.

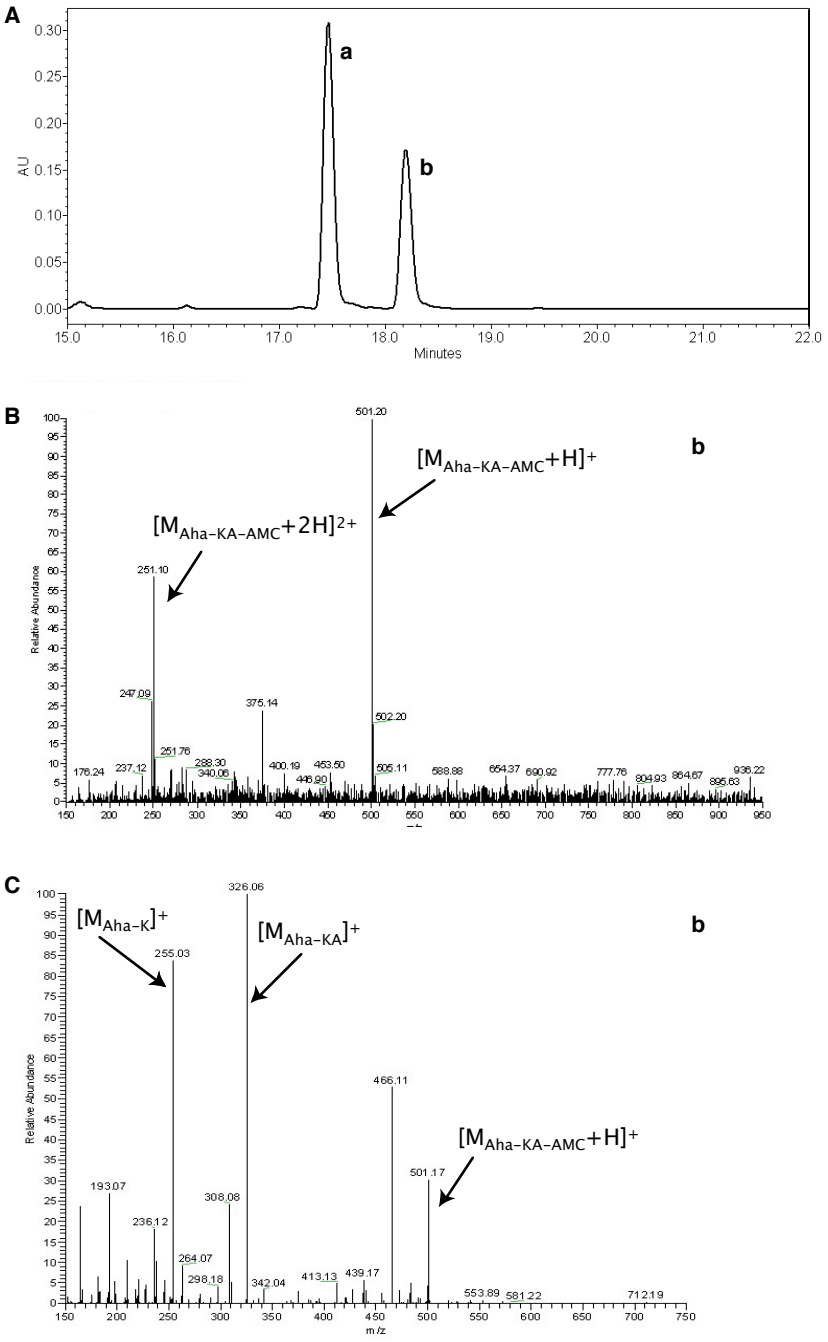

Figure A-21. (A) Representative reversed-phase HPLC analysis of the transfer reaction of azidohomoalanine **8** (Aha) to KA-AMC using UV detection at 324 nm. Both the starting material (a) and the tripeptide product (b) are visible. (B) Analysis of peak (b) by ESI mass spectrometry confirms that it contains the tripeptide product, Aha-KA-AMC, expected $[M_{Aha\text{-}KA\text{-}AMC}+H]^+$ = 501.25 *m/z* and $[M_{Aha\text{-}KA\text{-}AMC}+2H]^{2+}$ =251.13 *m/z*. (C)) MS/MS analysis of the singly-charged ion of the product further confirms the N-terminal addition of Aha to KA-AMC with fragmentation into dipeptide Aha-K, $[M_{Aha\text{-}K}]^+$=255.30 *m/z* and the tripeptide Aha-KA, $[M_{Aha\text{-}KA}]^+$= 326.19 *m/z*.

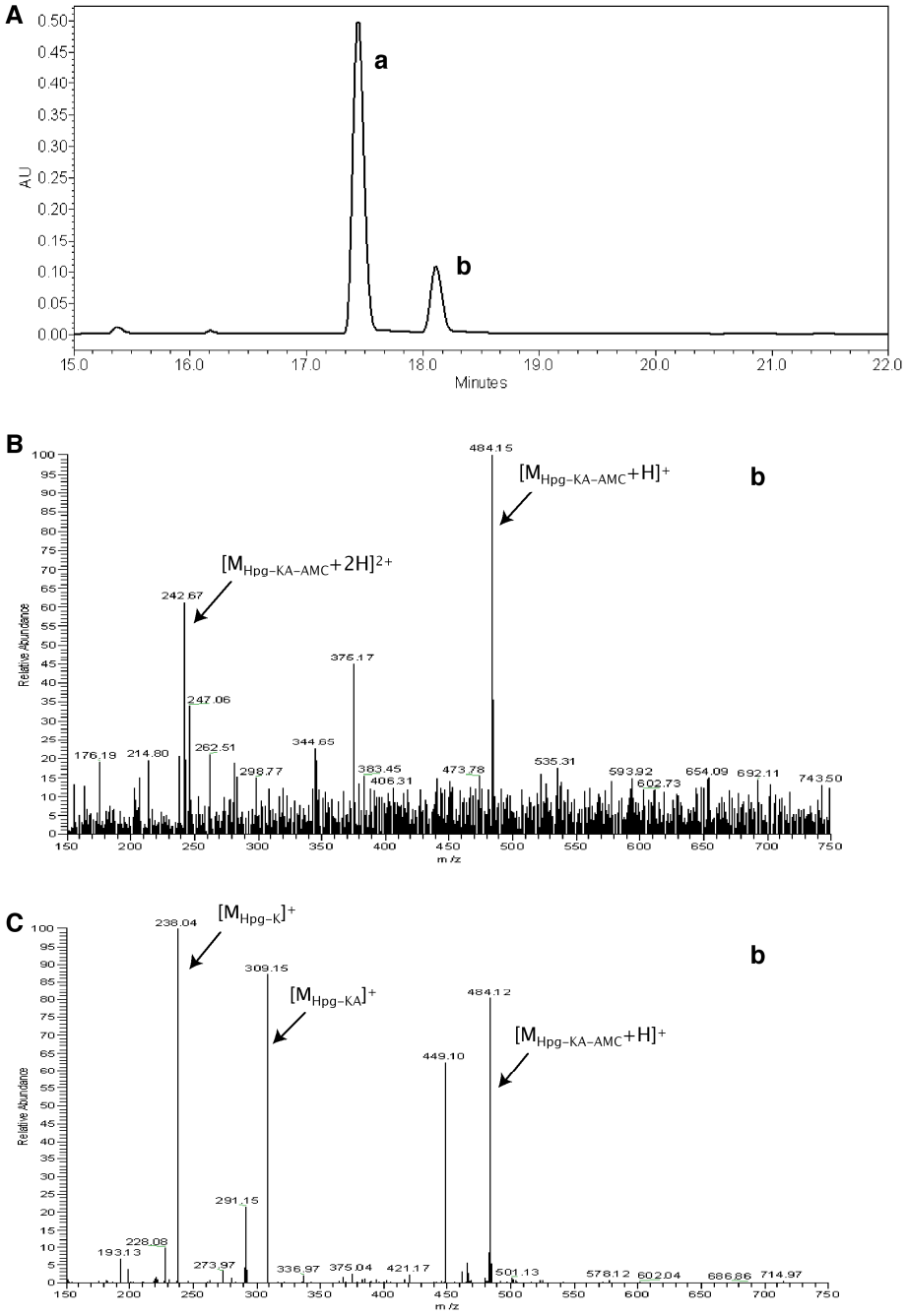

Figure A-22. (A) Representative reversed-phase HPLC analysis of the transfer reaction of homopropargylglycine **9** (Hpg) to KA-AMC using UV detection at 324 nm. Both the starting material (a) and the tripeptide product (b) are visible. (B) Analysis of peak (b) by ESI mass spectrometry confirms that it contains the tripeptide product, Hpg-KA-AMC, expected $[M_{Hpg\text{-}KA\text{-}AMC}+H]^+$=484.25 *m/z* and $[M_{Hpg\text{-}KA\text{-}AMC}+2H]^{2+}$ =242.63 *m/z*. (C) MS/MS analysis of the singly-charged ion of the product further confirms the N-terminal addition of Hpg to KA-AMC with fragmentation into dipeptide Hpg-K, expected $[M_{Hpg\text{-}K}]^+$=238.16 *m/z* and the tripeptide Hpg-KA, expected $[M_{Hpg\text{-}KA}]^+$= 309.19 *m/z*.

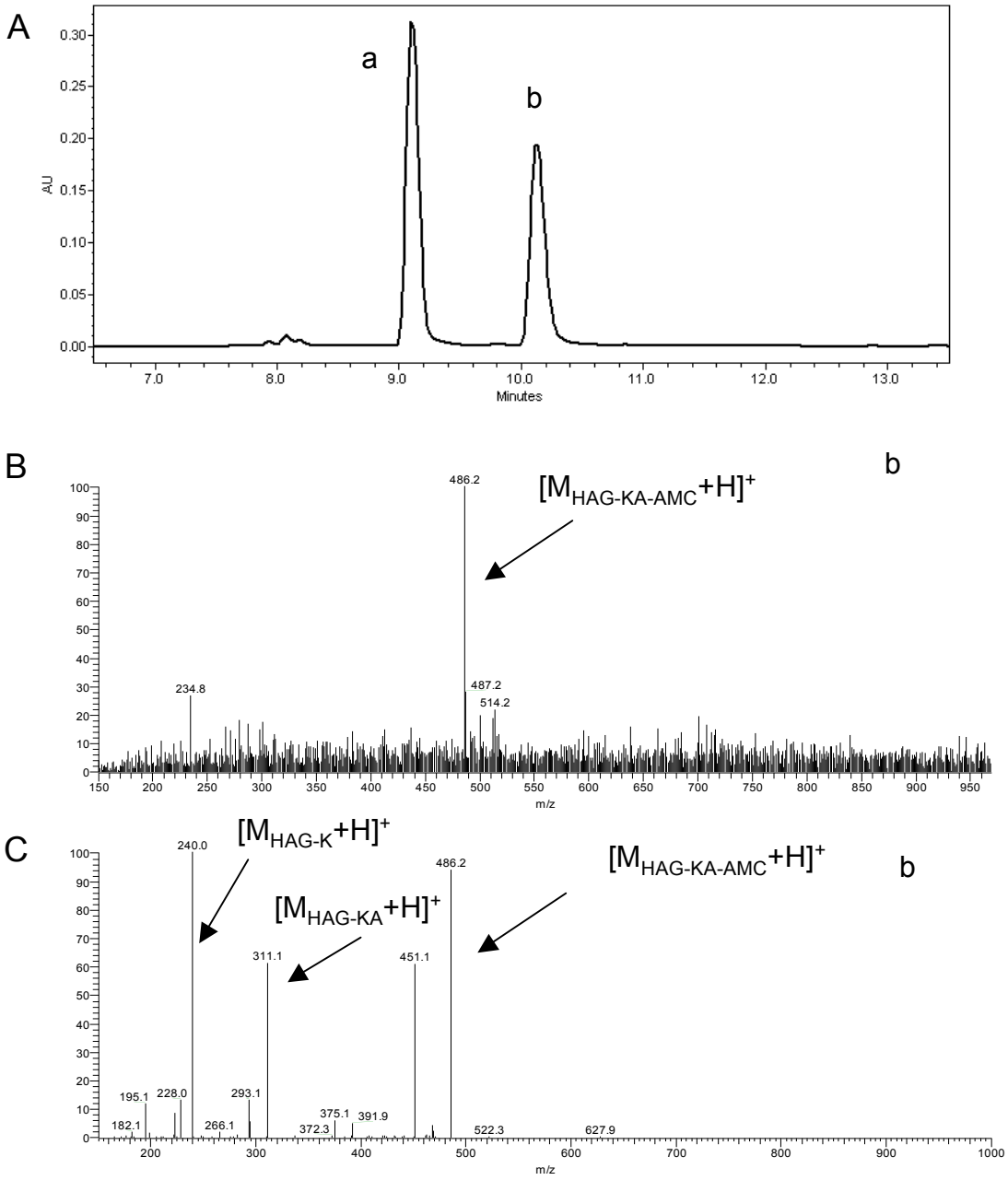

Figure A-23. (A) Representative reversed-phase HPLC analysis of the transfer reaction of homoallylglycine (HAG) to KA-AMC using UV detection at 324 nm. Both the starting material (a) and the tripeptide product (b) are visible. (B) Analysis of peak (b) by ESI mass spectrometry confirms that it contains the tripeptide product, HAG-KA-AMC, expected $[M_{HAG\text{-}KA\text{-}AMC}+H]^+$ = 486.2 *m/z.* (C) MS/MS analysis of the singly-charged ion of the product further confirms the N-terminal addition of HAG to KA-AMC with fragmentation into dipeptide HAG-K, expected $[M_{HAG\text{-}K}]^+$240.0 *m/z* and the tripeptide HAG-KA, expected $[M_{HAG\text{-}KA}]^+$= 311.1 *m/z*.

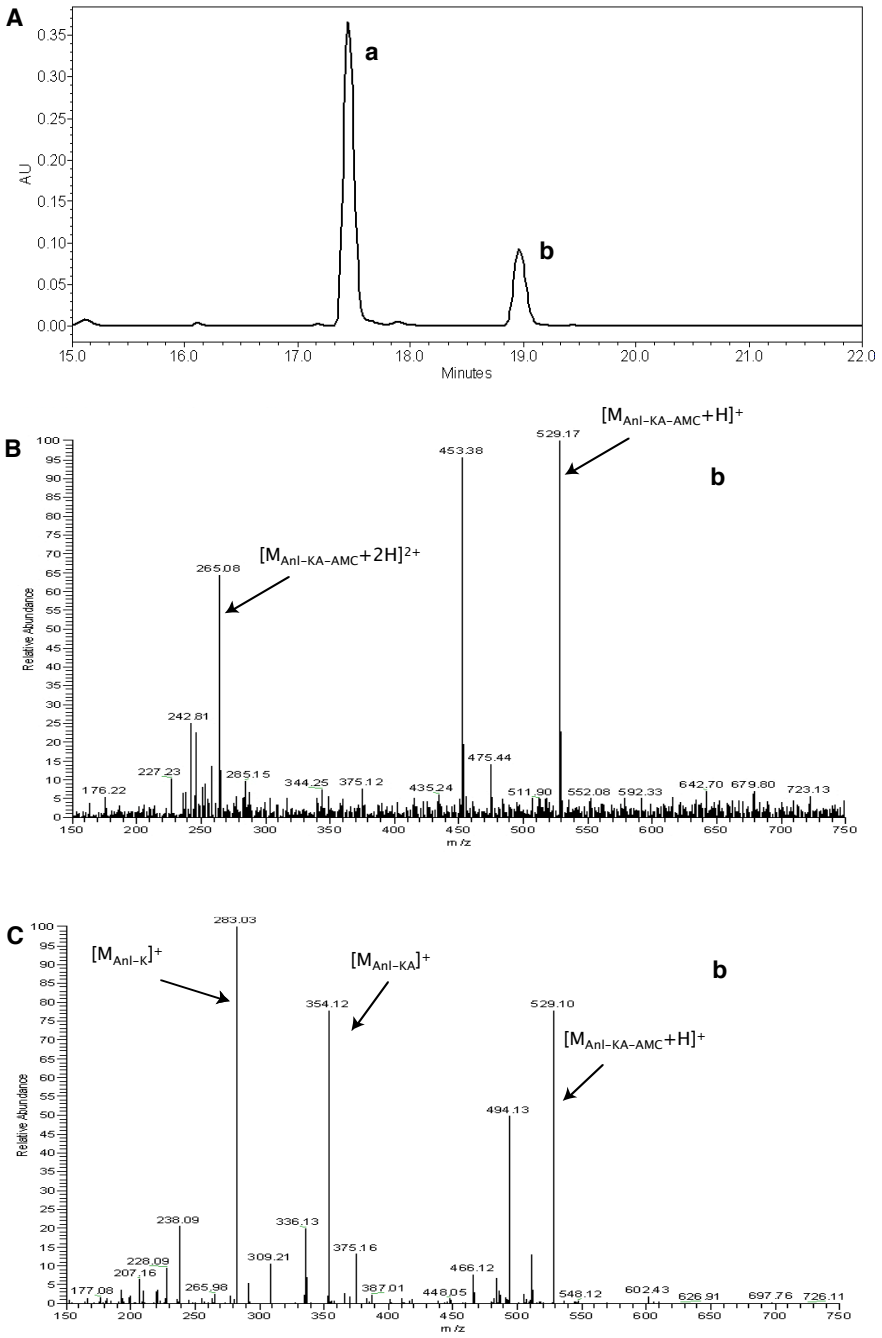

Figure A-24. (A) Representative reversed-phase HPLC analysis of the transfer reaction of azidonorleucine **10** (Anl) to KA-AMC using UV detection at 324 nm. Both the starting material (a) and the tripeptide product (b) are visible. (B) Analysis of peak (b) by ESI mass spectrometry confirms that it contains the tripeptide product, Anl-KA-AMC, expected $[M_{Anl\text{-}KA\text{-}AMC}+H]^+$ = 529.28 *m/z* and $[M_{Anl\text{-}KA\text{-}AMC}+2H]^{2+}$ = 265.14 *m/z*. (C) MS/MS analysis of the singly-charged ion of the product further confirms the N-terminal addition of Anl to KA-AMC with fragmentation into dipeptide Anl-K, expected $[M_{Anl\text{-}K}]^+$=283.19 *m/z* and the tripeptide Anl-KA, expected $[M_{Anl\text{-}KA}]^+$= 354.23 *m/z*.